AIP | Applied Physics Letters

Pulsed laser ablation of complex oxides: The role of congruent ablation and preferential scattering for the film stoichiometry

S. Wicklein, A. Sambri, S. Amoruso, X. Wang, R. Bruzzese et al.

Citation: Appl. Phys. Lett. **101**, 131601 (2012); doi: 10.1063/1.4754112
View online: http://dx.doi.org/10.1063/1.4754112
View Table of Contents: http://apl.aip.org/resource/1/APPLAB/v101/i13
Published by the American Institute of Physics.

Pulsed laser ablation of complex oxides: The role of congruent ablation and preferential scattering for the film stoichiometry

S. Wicklein,[1] A. Sambri,[2] S. Amoruso,[2] X. Wang,[2] R. Bruzzese,[2] A. Koehl,[1] and R. Dittmann[1]
[1]*Peter Grünberg Institut and JARA-FIT, Forschungszentrum Juelich GmbH, 52425 Juelich, Germany*
[2]*CNR-SPIN and Dipartimento di Scienze Fisiche, Complesso Universitario di Monte Sant'Angelo, Via Cintia, I-80125 Napoli, Italy*

(Received 18 July 2012; accepted 4 September 2012; published online 24 September 2012)

By combining structural and chemical thin film analysis with detailed plume diagnostics and modeling of the laser plume dynamics, we are able to elucidate the different physical mechanisms determining the stoichiometry of the complex oxides model material $SrTiO_3$ during pulsed laser deposition. Deviations between thin film and target stoichiometry are basically a result of two effects, namely, incongruent ablation and preferential scattering of lighter ablated species during their motion towards the substrate in the O_2 background gas. On the one hand, a progressive preferential ablation of the Ti species with increasing laser fluence leads to a regime of Ti-rich thin film growth at larger fluences. On the other hand, in the low laser fluence regime, a more effective scattering of the lighter Ti plume species results in Sr rich films. © *2012 American Institute of Physics*. [http://dx.doi.org/10.1063/1.4754112]

Complex transition metal oxides exhibit a large variety of interesting physical properties comprising high temperature superconductivity, piezoelectricity, ferroelectricity, magnetism, and multiferroicity. The observation of an electrically tuneable two dimensional electron gas at epitaxial heterointerfaces provides further device design opportunities for this class of materials.[1]

Due to the strong impact of slight deviations from the ideal stoichiometry on the physical properties of oxide thin films and heterostructures, the understanding and precise control over the formation of vacancy defects is one of the key challenges for the oxide thin film growth community. The significant role of acceptor-type cation vacancies in the suppression of the donor doping activity in $SrTiO_3$ (STO) was recently demonstrated.[2,3] Since the properties of the conducting $SrTiO_3/LaAlO_3$ heterointerfaces can be strongly modified by small variations of the $LaAlO_3$ stoichiometry,[4–6] the impact of cation vacancies became obvious also in the field of oxide-based research.

Pulsed laser deposition (PLD) is the most widely spread method for the growth of complex oxides, since it has been generally assumed in the past that above a certain laser fluence threshold the target stoichiometry is properly transferred to the thin film. However, in Ref. 7, it was demonstrated that the Sr/Ti ratio of homoepitaxially grown STO thin films strongly depends on the laser fluence, and that a stoichiometric transfer is only obtained for a certain laser fluence. The fluence dependence of the cation stoichiometry has also been recently confirmed for a variety of perovskite thin films.[4,8–11] Nonetheless, the physical mechanisms underlying this phenomenon has not yet been clarified up to now. In an early work,[12] the Ti deficiency of STO thin films grown at low laser fluences was attributed to a volume-diffusion-assisted preferential ablation process. However, the deviations from the target stoichiometry at higher laser fluence could not be explained within this model.

In this letter, we aim to clarify the origin of this generally observed fluence dependence of the thin film composition for the model material STO. This is achieved by carrying out systematic PLD growth conditions studies, where we combine the characterization of the STO plume with thin film chemical analysis via x-ray photoelectron emission spectroscopy (XPS).

By utilizing a KrF excimer laser (pulse width = 20 ns), STO thin films (thickness ≈200 nm) were grown homoepitaxially at a background oxygen pressure of 0.2 mbar, and a substrate surface temperature of 720 °C. The (001) STO substrates were annealed at 950 °C for 4 h in air prior to deposition to create a regular vicinal surface. Moreover, an analysis of the STO plume dynamics and composition was carried out by time- and space resolved imaging.

Figure 1 shows the deviation of the c-axis from the STO bulk value, Δc, as a function of the laser fluence, F, for three different values of the target to substrate distance, D_{TS}, (40,

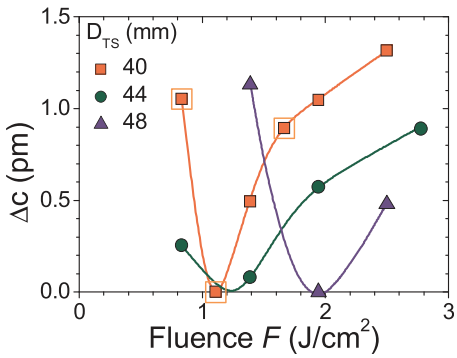

FIG. 1. c-axis expansion, Δc, of epitaxial STO thin films (≈200 nm) vs laser fluence, F, at three different target-to-substrate distances (D_{TS}) grown at a substrate temperature $T_S = 720$ °C in 0.2 mbar of oxygen background gas. The curves are visual guides. The orange squares mark the conditions for which XPS analyses of the thin films and of the corresponding ablation spots on the target were carried out.

44, and 48 mm). As reported earlier,[7,13] STO thin films exhibiting c-axis values of bulk STO can be regarded as stoichiometric, whereas thin films with expanded c-axis exhibit a significant non-stoichiometry. In particular, STO thin films grown at high laser fluence are Ti rich, whereas thin films grown at low laser fluence are Sr rich.[7,13] By employing positron annihilation lifetime spectroscopy, we explicitly demonstrated that Δc is induced by Sr and Ti vacancies for the high and low fluence regime, respectively.[8]

Figure 1 also exemplifies that at a given fluence, e.g., $F = 1.5\,\mathrm{J/cm^2}$, the films can be nearly stoichiometric ($D_{TS} = 44\,\mathrm{mm}$) but also extremely non-stoichiometric with a Ti-rich ($D_{TS} = 40\,\mathrm{mm}$) or a Sr-rich ($D_{TS} = 48\,\mathrm{mm}$) composition, depending on the target-to-substrate distance. This is a hint that the puzzling variation of the STO film stoichiometry results from an intricate combination between preferential scattering of light plume species, e.g., Ti in STO, during their flight towards the substrate[14] and incongruent ablation of the STO target that compensates for scattered species. Any influence of re-sputtering processes on the film stoichiometry can be excluded[15] due to the rather low kinetic energy of the plume species reaching the substrate located at a distance of several cm,[16] at a deposition pressure of $\approx 10^{-1}$ mbar. In the following, we illustrate our experimental results addressing such a scenario.

To analyze the stoichiometry of the films and the congruence of ablation, XPS analysis of the STO thin films and of the corresponding ablation spots on the STO target were carried out. This analysis was performed in the three experimental conditions marked by squares in Figure 1, corresponding to $D_{TS} = 40\,\mathrm{mm}$ and laser fluencies of 0.8, 1.1, and 1.7 J/cm.[2] The XPS results are summarized in Table I. It can be clearly seen that STO thin films exhibiting a c-axis expansion reveal a Sr/Ti ratio $\neq 1$. Films which show no c-axis expansion have a Sr/Ti ratio of ~ 1. In particular, films grown at low laser fluence show a Sr-rich composition, while those grown at high laser fluence exhibit a Sr/Ti ratio < 1, i.e., a Ti-rich composition. These findings are in agreement with the literature[7,13] and our earlier findings.[8]

Moreover, XPS analysis of the ablation spots was carried out. The spots exhibited the same morphology as in Ref. 29 and reveal that the Sr/Ti ratio on the STO target increases with increasing laser fluence. This indicates a preferential ablation of Ti species from the target for higher laser fluencies leaving behind a Sr-rich STO surface. The case of incongruent ablation of STO was reported earlier by Ref. 12 with the same observation that the Sr/Ti ratio of the ablation spot increases with laser fluence. This unidirectional trend of the Sr/Ti ratio on the target, however, does not explain the observed variation of the film stoichiometry with the target-to-substrate distance, at a fixed fluence (see Fig. 1), and the increase of the Sr/Ti ratio of the thin films deposited at $0.8\,\mathrm{J/cm^2}$ (Table I). It rather points to a preferential loss of the lighter Ti cation in the deposited film when the plume has to propagate over longer distances into the background gas to reach the substrate.

TABLE I. XPS analysis of the STO thin films and of the corresponding ablation spots of the STO single crystal target.

	Sr/Ti ratio	
F (J/cm^2)	Thin film	Target
0.8	1.15 ± 0.05	1.00 ± 0.05
1.1	1.00 ± 0.05	1.05 ± 0.05
1.7	0.80 ± 0.05	1.13 ± 0.05

In order to further assess these issues, an analysis of the STO plume dynamics and composition was carried out, by using time-resolved optical spectroscopy of the expanding plume (see Refs. 16–18, e.g., for a detailed description). In this analysis, a value of $D_{TS} = 33\,\mathrm{mm}$ was used in order to image the whole plume expansion from the target to the substrate in our experimental setup.

Fig. 2 depicts the emission spectra of the STO plume in the early stage of its expansion, when the plume front edge has reached a distance of ≈ 5 mm from the target surface and the influence of the background gas is still negligible, for three different values of the fluence F. The STO spectrum is very rich, presenting many lines in the visible region which namely belong to excited Sr and Ti atoms.[19] For the assignment of the different emission lines, ablation experiments of TiO_2 were also carried out in order to reliably identify the features belonging to the two target species (Sr and Ti). Sr emission features are predominant in the spectral regions 638-654 nm and 661–687 nm, meanwhile various Ti emission lines are identified in the region 427–457 nm. In the region 480–559 nm, intense emission lines of both species overlap and cannot be attributed to a single element. The sequence of spectra in Fig. 2 reveals that the relative intensity of the Ti emission actually increases with increasing laser fluence. Having in mind that the XPS data indicate an increase of the Sr concentration on the ablated target surface with increasing laser fluence (Table I), we assign this observation to a preferential ablation of Ti species from the target for higher laser fluencies, leaving behind a Sr-rich STO surface. This is at odds with Ref. 12 which proposes a preferential ablation of Sr based on the observation of a Sr rich ablation spot on the target. Moreover, the findings of Fig. 2 also support the viability of using the emission intensity ratio

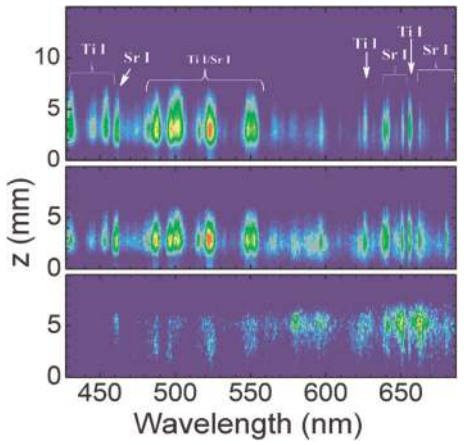

FIG. 2. (a) 1D spectra of the STO plume emission for three different values of the laser fluence, F: $0.6\,\mathrm{J/cm^2}$ (lower panel), $1.0\,\mathrm{J/cm^2}$ (middle panel), and $2.0\,\mathrm{J/cm^2}$ (upper panel). Each image is normalized to its own maximum intensity.

as a reliable, qualitative indication of the relative composition of the ablation plume.[20,21]

The transfer of ablated species from the target to the substrate can be influenced by different processes, which can eventually affect the film stoichiometry.[15] Among others, the joined effects of laser fluence, and plume-background gas interaction can be particularly relevant.[11,22] Fig. 3(a) reports single-shot images of the STO plume emission collected by an intensified-charge-coupled device (ICCD), at three different fluences, and for three succeeding temporal delays, τ, after the laser pulse. In Fig. 3(a), each image is normalized to its own maximum intensity, to facilitate the comparison. The plume propagation direction is along the z-axis, and $z=0$ marks the position of the target surface, while the x-axis is parallel to the target surface. From sequences of images such as those in Fig. 3(a), the temporal evolution of the plume front position, R, was obtained,[23] and shown in Fig. 3(b). This helps understanding the effect of the laser fluence on the plume propagation dynamics from the target to the substrate. The solid curves in Fig. 3(b) are fits according to the plume propagation model described in Refs. 16 and 23. This model uses a simple physical approach based on the balance between plume linear momentum variation and the external pressure force, and uses as fitting parameters the initial front velocity, u_0, and driving mass, M_p, of the plume (see Table II). The laser fluence F defines the initial driving energy of the ablated material through the amount of ablated species, and their initial velocity, and the corresponding plume propagation dynamics. By reducing the fluence, the initial driving energy of the STO plume decreases, and the braking effect of the background gas correspondingly increases. For low fluencies, the plume is significantly braked, eventually stopping before reaching the substrate. In this case, the plume species can reach the substrate only through diffusion into the background gas.[24] In such a regime, the diffusion-like flow of the plume species towards the substrate can be significantly non-stoichiometric as a consequence of the collisional processes between ablated species and background gas molecules.[15] On the contrary, an increase of the laser fluence progressively reduces the background gas confinement, and the plume impacts on the substrate at earlier times (see Fig. 3).

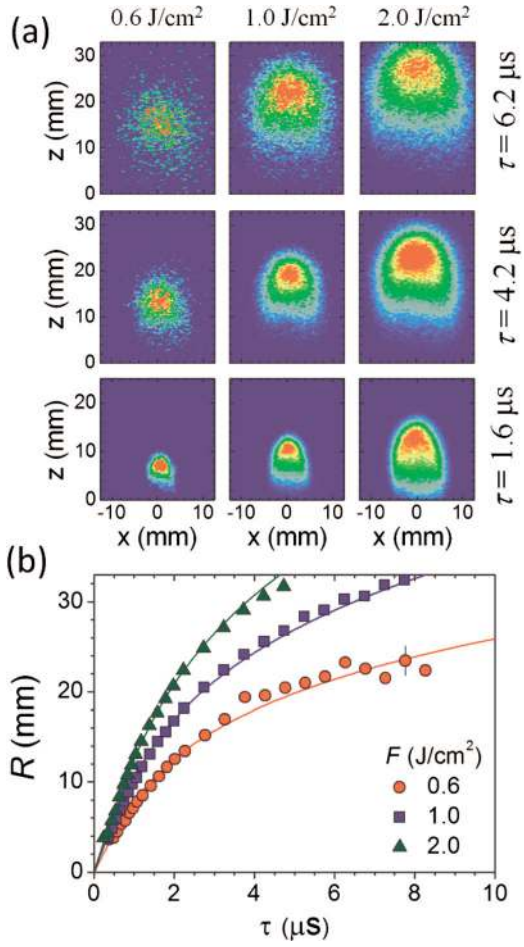

FIG. 3. (a) 2D images of the STO plume emission for three different values of the laser fluence, F, at three delays, τ, after the laser pulse. (b) Position-time R-τ plots of the plume front for the three different values of the laser fluence of Fig. 3(a). The solid lines are fits according to the expansion model of Refs. 16 and 23.

In the framework of a collisional scattering approach, a mean free path of few mm can be estimated, by resting on a typical (energy independent) cross section of $\approx 5 \times 10^{-16}$ cm^2.[25,26] This value can be even shorter for the ablated species located at the plume front, due to the increase of the background gas density consequent to the plume confinement.[27,28] Moreover, the confinement also influences the collisional dynamics of the inner plume species.[27] Thus, the plume species can suffer several collisions, both with the background gas molecules and among themselves, depending on the residual distance to the substrate, and time needed to reach it. In any scattering event, the lighter species diffuses to larger angles, resulting in an enhancement of heavier species (Sr for STO) along the direction normal to the substrate. This explains the larger content of Sr observed in the STO thin films deposited at lower fluences, even if the nascent plume is stoichiometric (see Table I). On the contrary, at larger fluencies, the confining effect of the background gas is strongly reduced: for example, in Fig. 3, at $F = 2.0$ J/cm^2, the plume expands rather freely reaching the substrate already at $\tau \approx 4.5\,\mu$s. In such a condition, the plume composition is closer to that of the nascent plume observed at short distance from the target surface, i.e., a Ti-rich plume. This, in turn, leads to a STO film characterized by a Sr/Ti ratio smaller than 1. At any fixed target-to-substrate distance, the intricate interplay between the progressive variation of the plume composition, due to the incongruent ablation of the STO target, and the transition from an halted to a progressively more free plume propagation, allows passing from Sr-rich to Ti-rich STO films, going from low to high fluence, with a stoichiometric deposition occurring at an intermediate fluence, as observed in Fig. 1.

TABLE II. Values of the initial front velocity, u_0, and driving mass, M_p, of the STO plume as a function of the laser fluence F, as obtained by fitting of the plume front dynamics to the model described in Refs. 16 and 23.

F (J/cm^2)	u_0 (km/s)	M_p (10^{-10} kg)
0.6	8 ± 1	3.1 ± 0.5
1.0	12 ± 2	6.5 ± 0.9
2.0	14 ± 2	13 ± 2

In the case of incongruent target ablation of complex oxides, as for STO, the results discussed above also indicate that, at a fixed oxygen background gas pressure, it is possible to compensate for a larger content of the lighter species in the nascent ablation plume (e.g., Ti in STO) by appropriately selecting the target-to-substrate distance. In an attempt to further elaborate on this issue, one can follow how the ratio of the emission intensity of Sr and Ti species, considered as a figure of the species predominance, changes with the thickness of the background gas layer crossed by the plume species during their propagation along the normal to the target surface and towards the substrate. In O_2, oxides formation significantly affects the plume emission features,[17,18] thus, influencing Sr/Ti emission intensity ratio, and shadowing any effect due to the propagation kinetics occurring during the plume-background gas interaction. Therefore, we decided to analyze STO propagation through an inert gas, which predominantly influences the species kinetics to study the effect of the Sr/Ti emission intensity ratio during the propagation phase in a background atmosphere. The STO ablation plume was produced at a laser fluence $F = 1.5\,\mathrm{J/cm^2}$ in ≈ 0.2 mbar of Ar. In these experiments, the substrate was held at room temperature. The registered STO plume spectra were analyzed and the total emission signal associated to Sr and Ti excited atoms reaching a fixed distance from the target surface, d, was evaluated. The variation of Sr/Ti emission intensity vs. d is shown in Fig. 4 (the value of the Sr/Ti intensity ratio at lower distances was fictitiously put equal to 1). The inset of Fig. 4 reports the position-time, $R - \tau$, plot of the STO plume propagation along the normal to the target surface, in Ar. We observe that as soon as the plume front brakes (see inset of Fig. 4) for $d \approx 8$–10 mm, the Sr/Ti emission intensity ratio starts to increase. At larger distances and later delays, the gradual braking of the plume expansion is associated to a further progressive increase of the Sr/Ti intensity ratio. This suggests that the interaction with the background gas increasingly leads to a predominance of the heavier species along the normal to the target surface, i.e., the direction to the substrate, which strongly supports the scenario proposed above to explain the fluence variation of the STO film stoichiometry.

In conclusion, we could clarify that the observed variation of the STO thin film stoichiometry with laser fluence, and target-to-substrate distance results from an intricate combination between preferential scattering of light plume species, e.g., Ti in STO, during the propagation towards the substrate and incongruent ablation of the STO. In particular, the Ti-rich films observed in the high fluence regime result from the increase of Ti-content in the plume due to the preferential ablation of the Ti species with increasing laser fluence. On the other side, the Sr-rich films obtained in the low fluence regime result from the loss of Ti-species during the transfer of the plume from the target to the substrate, rather than from a Sr rich ablation. In fact, the plume-background gas interaction, leading to the aforementioned scattering mechanism of the lighter species, is more effective in the low fluence regime. The loss of Ti-species at low fluence can in principle be compensated by reducing the target-to-substrate distance. Another approach could be to use an ablation target with an enriched content of the lighter species. Our findings are of general importance for the growth of complex oxides containing elements with significant difference in atomic weight, and open up the way for a more defined control of the deposited thin film stoichiometry.

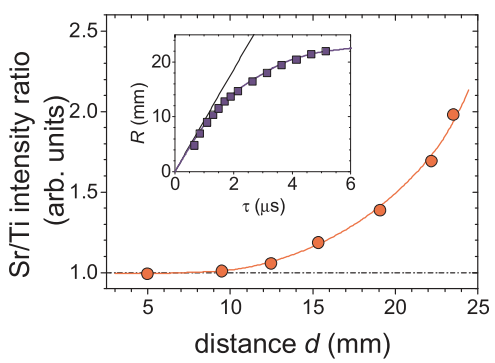

FIG. 4. Sr/Ti emission intensity ratio as a function of the distance from the target surface for laser ablation of STO in Ar background gas. The inset shows the temporal evolution of the plume front. The solid lines are visual guides to the eye.

The research has received funding from European Union Seventh Framework Programme (FP7/2007-2013) under Grant Agreement No. 264098—MAMA and the Deutsche Forschungsgemeinschaft (SFB 917). We thank C. Aruta and E. Di Gennaro for their valuable help.

[1]D. G. Schlom and J. Mannhart, Nature Mater. **10**, 168–169 (2011); J. Mannhart and D. G. Schlom, Science **327**, 1607–1611 (2010).
[2]J. Son, P. Moetakef, B. Jalan, O. Bierwagen, N. J. Wright, R. Engel-Herbert, and S. Stemmer, Nature Mater. **9**, 482–484 (2010).
[3]Y. Kozuka, Y. Hikita, C. Bell, and H. Y. Hwang, Appl. Phys. Lett. **97**, 012107 (2010).
[4]S. A. Chambers, Surf. Sci. **605**, 1133–1140 (2011).
[5]F. Schoofs, T. Fix, A. S. Kalabukhov, D. Winkler, Y. Boikov, I. Serenkov, V. Sakharov, T. Claeson, J. L. MacManus-Driscoll, and M. G. Blamire, J. Phys.: Condens. Matter **23**, 305002 (2011).
[6]P. Roy, C. Richter, J. Mundy, J. Ludwig, S. Paetel, T. Heeg, A. A. Pawlicki, L. Fitting Kourkoutis, M. Zheng, B. Mulcahy *et al.*, "La(1-δ)Al(1 + δ)O3 stoichiometry found key to electron liquid formation at LaAlO3/SrTiO3 interfaces," (submitted).
[7]T. Ohnishi, M. Lippmaa, T. Yamamoto, S. Meguro, and H. Koinuma, Appl. Phys. Lett. **87**, 241919 (2005).
[8]D. J. Keeble, S. Wicklein, R. Dittmann, R. Ravelli, R. A. Mackie, and W. Eder, Phys. Rev. Lett. **105**, 226102 (2010).
[9]D. Kan and Y. Shimakawa, Appl. Phys. Lett. **99**, 81907 (2011).
[10]E. Breckenfeld, R. Wilson, J. Karthik, A. R. Damodaran, D. G. Cahill, and L. W. Martin, Chem. Mater. **24**, 331 (2012).
[11]P. Orgiani, R. Ciancio, A. Galdi, S. Amoruso, and L. Maritato, Appl. Phys. Lett. **96**, 032501 (2010).
[12]B. Dam, J. H. Rector, J. Johansson, J. Huijbertse, and D. G. De Groot, J. Appl. Phys. **85**, 3386 (1997).
[13]T. Ohnishi, K. Shibuya, T. Yamamoto, and M. Lippmaa, J. Appl. Phys. **103**, 103703 (2008).
[14]T. E. Itina, W. Marine, and M. Autric, J. Appl. Phys. **82**, 3536 (1997).
[15]J. Schou, Appl. Surf. Sci. **255**, 5191 (2009).
[16]A. Sambri, S. Amoruso, X. Wang, M. Radovic', F. Miletto Granozio, and R. Bruzzese, Appl. Phys. Lett. **91**, 151501 (2007).
[17]S. Amoruso, C. Aruta, R. Bruzzese, D. Maccariello, L. Maritato, F. Miletto Granozio, P. Orgiani, U. Scotti di Uccio, and X. Wang, J. Appl. Phys. **108**, 043302 (2010).
[18]C. Aruta, S. Amoruso, R. Bruzzese, X. Wang, D. Maccariello, F. Miletto Granozio, and U. Scotti di Uccio, Appl. Phys. Lett. **97**, 252105 (2010).
[19]W. C. Martin, J. R. Fuhr, D. E. Kelleher, A. Musgrove, J. Sugar, W. L. Wiese, P. J. Mohr, and K. Olsen, *NIST Atomic Spectra Database (Version 2.0)* (National Institute of Standards and Technology, Gaithersburg, MD, 1999).

[20]R. C. Dye, R. E. Muenchausen, and N. S. Nogar, Chem. Phys. Lett. **181**, 531 (1991).
[21]P. Lecoeur, A. Gupta, P. R. Duncombe, G. Q. Gong, and G. Xiao, J. Appl. Phys. **80**, 513 (1996).
[22]J. Gonzalo, C. Afonso, and J. Perriere, J. Appl. Phys. **79**, 8042 (1996).
[23]A. Sambri, S. Amoruso, X. Wang, F. Miletto Granozio, and R Bruzzese, J. Appl. Phys. **104**, 053304 (2008).
[24]S. Amoruso, B. Toftmann, and J. Schou, Phys. Rev. E **69**, 056403 (2004).
[25]R. F. Wood, K. R. Chen, J. N. Leboeuf, A. A. Puretzky, and D. B. Geohegan, Phys. Rev. Lett. **79**, 1571 (1997).
[26]S. Amoruso, C. Aruta, R. Bruzzese, X. Wang, and U. Scotti di Uccio, Appl. Phys. Lett. **98**, 101501 (2011).
[27]N. Arnold, J. Gruber, and J. Heitz, Appl. Phys. A **69**, S87 (1999).
[28]T. E. Itina, J. Hermann, P. Delaporte, and M. Sentis, Phys. Rev. E **66**, 066406 (2002).
[29]L. M. Doeswijk, G. Rijnders, and D. H. A. Blank, Appl. Phys. A **78**, 263–268 (2004).